

Asymmetric Segregation of PIE-1 in *C. elegans* Is Mediated by Two Complementary Mechanisms that Act through Separate PIE-1 Protein Domains

Kimberly J. Reese,* Melanie A. Dunn,*
James A. Waddle,† and Geraldine Seydoux**

*Department of Molecular Biology and Genetics
School of Medicine
Johns Hopkins University
Baltimore, Maryland 21205

†Department of Molecular Biology and Oncology
University of Texas Southwestern
Medical Center at Dallas
Dallas, Texas 75230

Summary

The CCCH finger protein PIE-1 is a regulator of germ cell fate that segregates with the germ lineage in early embryos. At each asymmetric division, PIE-1 is inherited preferentially by the germline daughter and is excluded from the somatic daughter. We show that this asymmetry is regulated at the protein level by two complementary mechanisms. The first acts before cell division to enrich PIE-1 in the cytoplasm destined for the germline daughter. The second acts after cell division to eliminate any PIE-1 left in the somatic daughter. The latter mechanism depends on PIE-1's first CCCH finger (ZF1), which targets PIE-1 for degradation in somatic blastomeres. ZF1s in two other germline proteins, POS-1 and MEX-1, are also degraded in somatic blastomeres, suggesting that localized degradation also acts on these proteins to exclude them from somatic lineages.

Introduction

Asymmetric segregation of determinants during cell division is a commonly used mechanism to generate cell diversity during development. Regulatory molecules are segregated asymmetrically during mitosis to generate daughter cells with different intrinsic fates (Guo and Kemphues, 1996; Knoblich, 1997; Shapiro and Losick, 1997; Jan and Jan, 1998). For example, in *Drosophila* neuroblasts, the transcription factor Prospero is segregated preferentially to the basal daughter where it specifies the "ganglion mother cell" (GMC) fate by activating GMC-specific genes and inhibiting neuroblast-specific genes (Doe et al., 1991; Vaessin et al., 1991; Hirata et al., 1995; Knoblich et al., 1995). Similarly, in haploid cells of *S. cerevisiae*, the transcriptional repressor Ash1p accumulates preferentially in the newly budded daughter cell where it prevents mating type switching by inhibiting the expression of HO endonuclease (Bobola et al., 1996; Sil and Herskowitz, 1996). Although superficially similar, these two examples of asymmetric segregation are mediated by different mechanisms. In the case of Prospero, asymmetric segregation is dependent on a complex of cortical proteins that target Prospero to a crescent in the basal cortex of the dividing neuroblast.

This crescent is inherited by the basal daughter cell where Prospero is released from the cortex and enters the nucleus (Hirata et al., 1995; Knoblich et al., 1995). In contrast, asymmetric distribution of Ash1p depends on incorporation of the *ASH1* mRNA into cytoplasmic particles that travel through the mother cell toward the emerging bud tip. Ash1p is then translated at the bud tip where it translocates specifically into the daughter cell nucleus (Long et al., 1997; Takizawa et al., 1997; Bertrand et al., 1998).

Asymmetric segregation of determinants is also used during the first cleavages of the *C. elegans* embryo to generate distinct somatic and germ lineages. The zygote undergoes four asymmetric divisions, each of which gives rise to a larger somatic blastomere (AB, EMS, C, and D) and a smaller germline blastomere (P_1 , P_2 , P_3 , and P_4 ; Figure 1A). During these divisions, P granules and proteins required for germline development are inherited preferentially by the germline daughter and are excluded from the somatic daughter (Strome and Wood, 1982; Mello et al., 1996; Guedes and Priess, 1997; Tabara et al., 1998). P granules are large ribonucleoprotein complexes found exclusively in the germline (Strome and Wood, 1982; Pitt et al., 2000). Observation of fluorescently labeled P granules in live embryos revealed that in the zygote, P granule segregation involves both directed movement and localized degradation (Hird et al., 1996). Before the first cleavage, P granules scattered throughout the cytoplasm migrate toward the posterior pole where the germline blastomere P_1 will form; P granules that remain in the anterior are degraded (or disassembled). The molecular mechanisms underlying these behaviors are not known. P granule components that regulate movement or stability have not yet been identified. The actin cytoskeleton and several cortical proteins asymmetrically localized along the anterior/posterior axis are required for P granule segregation (Rose and Kemphues, 1998), but it is not known how these factors interact with the cytoplasmic P granules.

Another factor that segregates with the germ lineage in early embryos is PIE-1. PIE-1 is a maternally encoded protein required to inhibit mRNA transcription and somatic development in germline blastomeres (Mello et al., 1992, 1996; Seydoux et al., 1996). Like P granules, PIE-1 protein is initially found throughout the cytoplasm of newly fertilized embryos and becomes enriched in the posterior cytoplasm before the first cleavage (Mello et al., 1996; Tenenhaus et al., 1998). As a result, PIE-1 is inherited predominantly by P_1 in the 2-cell stage. Asymmetric segregation of PIE-1 is repeated in the germline blastomeres P_1 , P_2 , and P_3 . In contrast in P_4 , which divides equally and segregates P granules to both its descendants (Z2 and Z3), PIE-1 remains uniform and is partitioned equally to both daughters (Mello et al., 1996).

The mechanisms that regulate PIE-1 localization are not known. In principle, these mechanisms could act on the *pie-1* RNA, the PIE-1 protein, or both. Like many maternal RNAs, the *pie-1* RNA is maintained uniformly in all blastomeres until the 4-cell stage. After the 4-cell stage, it is lost from somatic blastomeres and retained only in germline blastomeres (Tenenhaus et al., 1998). RNA localization is therefore unlikely to contribute to PIE-1 localization before the 4-cell stage but could be

† To whom correspondence should be addressed (e-mail: gseydoux@jhmi.edu).

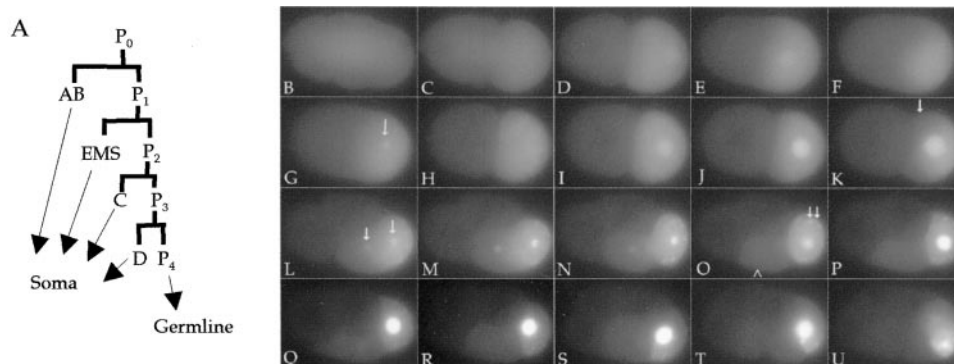


Figure 1. PIE-1 Dynamics In Vivo

(A) The zygote (P_0) undergoes a series of asymmetric cleavages (horizontal lines) to generate four somatic blastomeres (AB, EMS, C, and D) and successive germline blastomeres (P_1 , P_2 , P_3 , and P_4).

(B) In vivo visualization of PIE-1:GFP dynamics using time-lapse fluorescence microscopy. An embryo expressing wild-type PIE-1:GFP was examined by time-lapse imaging from the 1-cell stage to the 8-cell stage (birth of C and P_3) as described in Experimental Procedures. (B)–(U) are representative frames taken approximately every 2 min: B–H, 1-cell; I–M, 2-cell; N–P, 4-cell; Q–U, 6/8-cell. A QuickTime version of this movie can be seen at www.molecule.org/cgi/content/full/6/2/445/DC1.

Arrows point to the posterior centrosome in (G), clearing of PIE-1:GFP on the somatic side in (K), centrosomes in (L), and P granules in (O). Arrowhead in (O) points to low levels of PIE-1:GFP in EMS.

In this and all subsequent figures, embryos are oriented with anterior to the left and posterior to the right. Embryos are approximately 45 μm in length.

involved in later stages. Localized translation of the *pie-1* message could also be used to target PIE-1 to the germ lineage. Translational control has been shown to regulate the distributions of GLP-1 and PAL-1, two other maternally encoded proteins that are asymmetrically localized in early *C. elegans* embryos (Evans et al., 1994; Hunter and Kenyon, 1996). Neither of these proteins, however, is localized in the same pattern as PIE-1: GLP-1 is present in AB-derived blastomeres, and PAL-1 is present in P1-derived somatic and germline blastomeres.

Another possibility is that PIE-1 segregation is regulated by mechanisms that act directly on the PIE-1 protein. In particular, it has been suggested that PIE-1's ability to associate with centrosomes during mitosis may contribute to its asymmetric distribution (Mello et al., 1996). At the beginning of each mitosis, PIE-1 accumulates around both centrosomes of the nascent spindle. As the spindle rotates in preparation for cleavage, PIE-1 disappears from the centrosome destined for the somatic daughter ("somatic centrosome") and is retained only on the centrosome destined for the germline daughter ("germline centrosome") (Mello et al., 1996). After spindle rotation, somatic and germline centrosomes adopt different morphologies (Hyman and White, 1987) and could conceivably affect PIE-1 binding or stability differentially.

To distinguish between these possibilities and begin to identify the mechanisms that localize PIE-1, we have analyzed PIE-1 segregation in live embryos and have identified the domains within PIE-1 responsible for its localization. Our results indicate that PIE-1 asymmetry is regulated at the protein level but does not depend on binding to centrosomes. Instead, we show that PIE-1 segregation is regulated by two independent mechanisms that act before and after cell division to enrich PIE-1 in germline blastomeres and eliminate it from somatic blastomeres.

Results

PIE-1:GFP in Live Embryos

To examine PIE-1 localization in live embryos, we constructed a fusion between *pie-1* coding sequences and GFP (green fluorescent protein, [Chalfie et al., 1994]). This fusion (Table 1, A) is functional, as it can rescue the embryonic lethality of a *pie-1(0)* mutant (data not shown). In all 14 lines examined, GFP fluorescence in the adult germline and in embryos was observed in a pattern identical to that reported for PIE-1 using immunolocalization (Mello et al., 1996; Tenenhaus et al., 1998). In embryos, PIE-1:GFP was found predominantly in the cytoplasm and nuclei of germline blastomeres (Figure 1, B–U). In the cytoplasm, PIE-1:GFP was present both diffusely throughout the cytosol and at higher concentration on P granules (arrows in Figure 1, O, and data not shown). PIE-1:GFP also appeared to associate with discrete foci in nuclei (data not shown). The identity of these foci is not known.

To examine the dynamics of PIE-1 localization, we performed time-lapse imaging on live embryos expressing PIE-1 GFP over several cell divisions (Figure 1, B–U). In oocytes and newly fertilized embryos, PIE-1:GFP was present uniformly throughout the cytoplasm (data not shown and Figure 1B). In the late 1-cell stage after the pronuclei have formed, PIE-1:GFP levels began to decrease in the anterior and increase in the posterior (Figure 1C). By pronuclear meeting, PIE-1:GFP was found predominantly in the posterior (Figure 1E). During mitosis, PIE-1:GFP also accumulated on both centrosomes with higher levels on the posterior centrosome (arrow in Figure 1G). As a result of this asymmetric enrichment, most of the PIE-1:GFP was inherited by the posterior blastomere P_1 during the first cleavage (Figure 1H).

In P_1 , P_2 , and P_3 , PIE-1:GFP distribution followed a sequence similar to that observed in the zygote, with the exception that PIE-1:GFP became increasingly more nuclear during each interphase (compare panels J and

Table 1. Identification of Domains in PIE-1 Required for Localization

	Construct	Genotype	Centrosomes	Nucleus	P granules	Enrichment before division	Elimination from soma after division	# of lines
A	Wild-type 	<i>pie-1(+)</i> <i>pie-1(0)</i>	+	+	+	+	+	14
			+	+	+	+	+	1
B		<i>pie-1(+)</i> <i>pie-1(0)</i>	+	+	+	+	+	3
			+	+	+	+	+	1
C		<i>pie-1(+)</i>	+	+	+	+	+	3
			+	+	+	+	+	3
D		<i>pie-1(+)</i>	-	-	-	-	-	6
E		<i>pie-1(+)</i>	+	-	-	-	-	5
F		<i>pie-1(+)</i>	+	-	-	-	-	17
G		<i>pie-1(+)</i> <i>pie-1(0)</i>	+	reduced	+	+	+	7
			-	reduced	+	+	+	1
H		<i>pie-1(+)</i>	-	-	-	-	+	11
I		<i>pie-1(+)</i>	-	-	-	-	-	4
J		<i>pie-1(+)</i> <i>pie-1(0)</i>	-	-	-	-	+	9
			-	-	-	-	+	4
K		<i>pie-1(+)</i>	-	-	-	-	-	9
L		<i>pie-1(+)</i> <i>pie-1(0)</i>	+	+	+	+	-	7
			+	+	+	+	-	1
M		<i>pie-1(+)</i>	+	+	+	+	-	6
N		<i>pie-1(+)</i> <i>pie-1(0)</i>	-	-	+	+	-	6
			-	-	+	+	-	2
O		<i>pie-1(+)</i> <i>smg-1*</i>	-	-	-	-	-	1
P		<i>pie-1(+)</i>	-	-	-	-	-	7
Q		<i>pie-1(+)</i>	-	-	+	-	-	10
R		<i>pie-1(+)</i>	-	-	+	-	-	6
S		<i>pie-1(+)</i>	-	-	+	-	-	9
T		<i>pie-1(+)</i> <i>pie-1(0)</i>	+	+	reduced	-	+	13
			+	+	reduced	-	+	1
U		<i>pie-1(+)</i>	+	+	+	+	+	5
V		<i>pie-1(+)</i>	+	+	+	reduced	+	5
W		<i>pie-1(+)</i>	+	+	+ or reduced#	reduced	+	2
			+	+	+ or reduced#	reduced	+	2
X		<i>pie-1(+)</i>	+	+	+	reduced	+	4
Y		<i>pie-1(+)</i> <i>pie-1(0)</i>	+	+	reduced	reduced	-	5
			+	+	reduced	reduced	-	1
Z		<i>pie-1(+)</i>	+	+	reduced	-	-	8

The constructs shown were transformed into *pie-1(+)* or *pie-1(0)* hermaphrodites, and their localization patterns were analyzed in live embryos. Boxes indicate PIE-1 coding regions and thin lines indicate *pie-1* noncoding regions (introns were omitted for clarity). All constructs were tagged with GFP at either the amino or carboxyl terminus as described in Experimental Procedures. In K and O, the *pie-1* coding region was present out-of-frame with respect to GFP. The following criteria were used to score the localization pattern of each fusion: centrosomes, GFP on two donut-shaped structures associated with mitotic nuclei as shown in Figure 1L. Nuclei, higher levels of GFP in interphase nuclei compared to surrounding cytoplasm in 2-cell and older embryos; "reduced" indicates a reduction in nuclear GFP levels compared to wild type. P granules, GFP on punctate structures in the cytoplasm as shown in Figure 1, O; "reduced" indicates that these structures were absent from interphase cells but could still be seen faintly in mitotic cells. Enrichment before division, higher levels of GFP on the germline side of dividing germline blastomeres compared to the somatic side (e.g., Figures 1D, 1L, and 3G); "reduced" indicates the presence of higher levels of GFP in the somatic daughter immediately after division compared to wild type. Elimination after division, absence of GFP in the daughters of AB, EMS, C, and D. (*) This construct could not be expressed in N2 hermaphrodites (data not shown) due to nonsense-mediated mRNA decay, which eliminates messages with abnormally long 3' UTRs. Therefore, we examined this construct in *smg-1* hermaphrodites where nonsense-mediated mRNA decay is inhibited (Pulak and Anderson, 1993). (#) This fusion was expressed at too low levels to determine whether it bound to P granules with normal affinity.

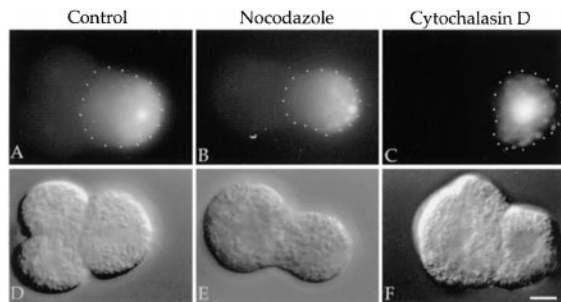


Figure 2. Effects of Actin and Microtubule Depolymerizing Drugs on PIE-1:GFP Localization

Fluorescence (A–C) and Nomarski (D–F) images of embryos expressing wild-type PIE-1:GFP. Embryos were treated with medium only (control, A and D), nocodazole (B and E), or cytochalasin D (C and F) as described in Experimental Procedures. The dotted lines in the fluorescence micrographs indicate the outline of P_1 . In 5/5 control embryos, PIE-1 became localized to the posterior of P_1 by the time AB had divided. Similarly, in 10/10 embryos treated with nocodazole, PIE-1 became localized to the posterior of P_1 by the time AB had attempted division and failed. In contrast, in 10/10 embryos treated with cytochalasin D, PIE-1 remained uniformly distributed in P_1 even after the AB nucleus had completed division. Scale bar is 10 μ m.

P in Figure 1). Before each cell division, PIE-1:GFP in the cytoplasm decreased on the side of the cell destined for the next somatic blastomere (“somatic side”, arrow in Figure 1K). At the start of mitosis, PIE-1:GFP disappeared from the nucleoplasm and became associated with centrosomes at both ends of the newly formed spindle (arrows in Figure 1L). As mitosis progressed, PIE-1:GFP levels in the cytoplasm continued to decrease on the somatic side of the cell; concomitantly PIE-1:GFP levels decreased on the centrosome destined for the somatic daughter and increased on the centrosome destined for the germline daughter (Figure 1M). After cytokinesis, most PIE-1:GFP was found in the germline daughter with only low levels left in the somatic daughter (e.g., EMS in the 4-cell stage, arrowhead in Figure 1, O). PIE-1:GFP fluorescence diminished progressively in that cell and was not detected in its progeny (Figure 1, O–U). These observations suggest that PIE-1 segregation to the germ lineage involves mechanisms that act both before cell division (to enrich PIE-1 on the germline side of the cell) and after cell division (to eliminate any PIE-1 remaining in the somatic daughter).

Asymmetric Enrichment before Cell Division Is Sensitive to Cytochalasin D but Not to Nocodazole

Segregation of P granules in the 1- and 2-cell stages requires an intact actin cytoskeleton (sensitive to cytochalasin D) but does not require intact microtubules (insensitive to nocodazole) (Strome and Wood, 1983; Hird et al., 1996). To determine whether PIE-1 segregation has similar requirements, we cultured 2-cell embryos expressing PIE-1:GFP in medium containing either cytochalasin D or nocodazole, following established procedures (Strome and Wood, 1983; Edgar, 1995; Shelton and Bowerman, 1996; Schlesinger et al., 1999). Both drugs blocked cell division as expected, but only cytochalasin D blocked PIE-1 enrichment to the posterior (Figure 2). These results indicate that like P

granules, PIE-1 requires an intact actin cytoskeleton to become enriched in the posterior before cell division. These experiments also suggest that intact microtubules may not be essential for this process. However, we cannot rule out their possible involvement since it was not possible to eliminate all microtubules with nocodazole (data not shown), as has also been noted by others (Strome and Wood, 1983).

Noncoding Sequences in the *pie-1* RNA are neither Necessary nor Sufficient for Segregation of the PIE-1 Protein to the Germ Lineage

To determine which sequences in *pie-1* are required for localization, we generated modified versions of the PIE-1:GFP fusion and analyzed their expression in vivo (Table 1). We began by testing the role of noncoding sequences, since these sequences are often implicated in RNA localization and translation control, two commonly used mechanisms for restricting the distribution of maternal proteins in embryos (Stebbins-Boaz and Richter, 1997; Lasko, 1999).

We first replaced the 3' UTR of *pie-1* with that of a *let-858*, a ubiquitously expressed gene (Kelly et al., 1997). This change did not affect PIE-1:GFP's ability to segregate asymmetrically (Table 1, B), though expression levels were reduced compared to wild-type (data not shown). Asymmetric segregation of the PIE-1:GFP:*let-858* 3' UTR fusion was not dependent on endogenous PIE-1 since it was also observed in a *pie-1(0)* mutant background (Table 1, B). We conclude that the *pie-1* 3' UTR is not essential for asymmetric segregation. To test other noncoding sequences, we placed the *pie-1* ORF fused to the *let-858* 3' UTR under the control of the *ama-1* promoter (Table 1, C). *ama-1* encodes the large subunit of RNA polymerase II and is expressed in all cells (Bird and Riddle, 1989). In this construct, the *pie-1* 5' UTR is replaced with that of *ama-1*, and the only sequences from the *pie-1* gene are coding sequences. Again, in this context PIE-1:GFP's ability to segregate to the germline was not affected (Table 1, C). To test the role of sequences in the *pie-1* open reading frame, we removed *pie-1* coding sequences from the original PIE-1:GFP fusion, leaving GFP in the context of the *pie-1* promoter and 5' and 3' UTRs. GFP expressed from this construct was no longer localized and was found at equal levels in all embryonic blastomeres (Table 1, D). We conclude that noncoding sequences are neither necessary nor sufficient for localization and that *pie-1* coding sequences contain all the information required.

Two Separate Domains in PIE-1 Are Required for Localization to the Germ Lineage

To identify domains in PIE-1 required for localization, we divided the *pie-1* open-reading frame into three segments (regions 1, 2, and 3) and tested each one individually for its ability to localize GFP in embryos.

Region 1

Fusion of region 1 (amino acids 1–84) to GFP caused GFP to accumulate at equal levels in the cytoplasm of all blastomeres with no preference for germline blastomeres (Table 1, E). In dividing cells, the region 1:GFP fusion became localized around centrosomes (both somatic and germline centrosomes were targeted equally; data not shown). The domain responsible for this localization was narrowed down to 21 amino acids (64–84, Table 1, F). A PIE-1:GFP fusion with this domain deleted

(PIE-1:GFP^{CenΔ}; Table 1, G) still bound to centrosomes, albeit with apparently reduced affinity (data not shown). We found that this localization is dependent on the presence of endogenous PIE-1. When expressed in a *pie-1(0)* background, PIE-1:GFP^{CenΔ} was no longer detected on centrosomes (Table 1, G). In both *pie-1(+)* and *pie-1(0)* embryos, however, PIE-1:GFP^{CenΔ} mutant segregated normally to germline blastomeres, although its accumulation in interphase nuclei appeared reduced compared to wild type (Table 1, G and data not shown). We conclude that the centrosome binding domain of PIE-1 is not required for asymmetric localization but may be required for efficient accumulation in nuclei.

Region 2

Fusion of region 2 (amino acids 85–173) to GFP caused GFP to accumulate preferentially in germline blastomeres and their sisters (Table 1, H). Deletion and mutational analysis of region 2 showed that a 36 amino acid domain encompassing the CCCH finger (ZF1, amino acids 97–132) was necessary and sufficient for this pattern when fused in-frame with GFP (Table 1, I and J) but not when fused out-of-frame (Table 1, K). In the zygote, ZF1:GFP remained uniformly distributed throughout the cytoplasm and was partitioned equally to AB and P₁ (Figure 3C). In the late 2-cell stage, ZF1:GFP levels remained high in P₁ but decreased in AB. In the 4-cell stage, the fusion was present at equal levels in the two P₁ daughters (EMS and P₂) but was much reduced or absent in the two AB daughters (ABa and ABp) (Figure 3D). This pattern of equal partitioning to both daughters during division followed by elimination from the somatic daughter and its progeny after division was repeated at each asymmetric cleavage. These results suggest that ZF1 is responsible for targeting PIE-1 for degradation in somatic blastomeres. Consistent with this interpretation, Cys-to-Ser mutations in (or deletion of) ZF1 in full-length PIE-1:GFP caused low levels of the fusion to be maintained in somatic blastomeres (Table 1, L and M; Figures 3E and 3F). Like wild-type, the ZF1 mutants became enriched on the germline side of the cell before each asymmetric division and were segregated preferentially to the germline daughter with only low levels inherited by the somatic daughter. Unlike wild type, however, the ZF1 mutants were not eliminated from the somatic daughter and instead persisted in its descendants (Figure 3F). We obtained direct evidence that ZF1 mutants are impaired in degradation by quantifying GFP fluorescence over time in embryos expressing wild-type and ZF1-mutated PIE-1:GFP fusions (Figure 4). In particular, we found that during the lifetime of EMS, wild-type PIE-1:GFP fluorescence decreased on average by 71% compared to 15% for the ZF1 mutant (Figure 4B). We conclude that, although not essential for asymmetric enrichment *before* cleavage, ZF1 is required to destabilize PIE-1 in somatic blastomeres *after* cleavage.

Region 3

Fusion of region 3 (amino acids 174–335) to GFP was sufficient to target GFP preferentially to germline blastomeres (Table 1, N). Before each asymmetric division, region 3:GFP became enriched on the germline side of the cell (Figure 3G) and was segregated preferentially to the germline daughter during cleavage (Figure 3H). This pattern was observed in both *pie-1(+)* and *pie-1(0)* embryos and was dependent on region 3 being fused in-frame to GFP (Table 1, N and O). A PIE-1:GFP fusion lacking most of region 3 (Table 1, T) remained uniform before cleavage and was partitioned equally to both

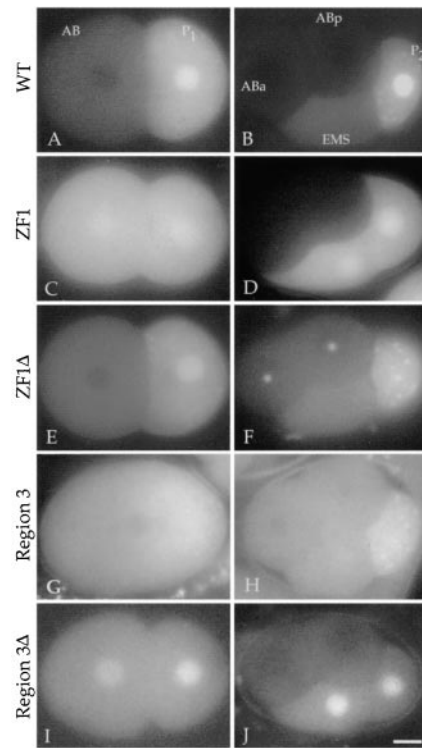


Figure 3. Two Nonoverlapping Domains in PIE-1 Are Required for Asymmetric Segregation

(A and B) Embryos expressing wild-type PIE-1:GFP (Table 1, A). Immediately after the first cleavage (A), high levels of PIE-1:GFP are present in P₁ and low levels are present in AB. In the 4-cell stage (B), PIE-1:GFP is detected in both P₁ daughters (EMS and P₂) but is no longer detected in the AB daughters (ABa and ABp).

(C and D) Embryos expressing ZF1:GFP (Table 1, J). This fusion is segregated equally to both daughters at the first cleavage (C) but is not maintained in AB descendants (D).

(E and F) Embryos expressing a PIE-1:GFP fusion missing ZF1 (Table 1, L). This fusion is segregated preferentially to P₁ at the first cleavage (E) and to P₂ in the second cleavage (F). However, low levels inherited by AB are maintained in its daughters (on centrosomes, [F]).

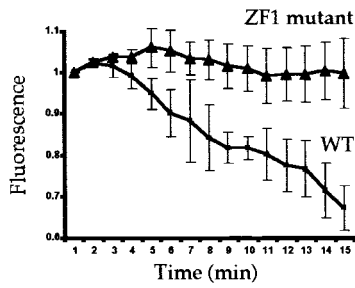
(G and H) Embryos expressing GFP fused to region 3 (Table 1, N). This fusion becomes enriched in the posterior before the first cleavage (G) and segregates preferentially to P₂ in the second cleavage (H). Low levels inherited by AB are maintained in its daughters (H).

(I and J) Embryos expressing a PIE-1:GFP fusion with a deletion in region 3 (Table 1, T). This fusion is segregated equally to both daughters during the first and second cleavages (I and J) but is not maintained in AB descendants (J). This fusion appears to have an increased nuclear-cytoplasmic ratio compared to other PIE-1:GFP fusions, suggesting that sequences in region 3 are also required to maintain high levels of PIE-1 in the cytoplasm of early embryos. Scale bar is 10 μm.

daughters (Figure 5I). This fusion, however, was not maintained in somatic blastomeres, indicating that it retained the ability to be degraded specifically in these cells (Figure 5J). We conclude that region 3 is necessary and sufficient for asymmetric enrichment before cleavage but is not required for elimination from somatic blastomeres after cleavage.

In germline blastomeres, region 3:GFP was found diffusely throughout the cytoplasm and on P granules (Figures 3G and 3H). Deletion analysis of region 3 showed

A. Total embryo



B. EMS

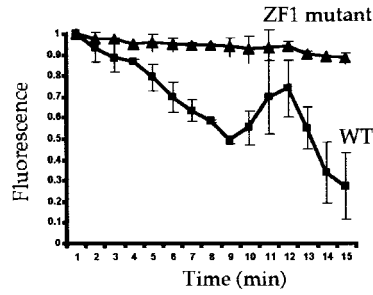


Figure 4. Quantification of ZF1-Dependent Degradation in Living Embryos

GFP fluorescence levels from three-dimensional time-lapse movies of embryos expressing either wild-type PIE-1::GFP (squares) or ZF1 mutant PIE-1::GFP (triangles). Plots compare the fraction of GFP fluorescence (y axis) relative to the first time point in a three-dimensional volume bounding the entire embryo (A) or the EMS cell (B) over time (x axis, minutes) starting at telophase of P1 (birth of EMS) and ending at telophase of EMS. Error bars indicate the 95% confidence limits in the mean values (see Experimental Procedures).

that the CCCH finger within this region (ZF2) is sufficient to target GFP to P granules (Table 1, R; Figure 6B). ZF2, however, was not sufficient to target GFP preferentially to germline blastomeres, suggesting that association with P granules is not sufficient for asymmetric segregation. Surprisingly, Cys/His to Ser mutations in ZF2 did not affect P granule binding significantly (Table 1, S and X). These mutations, however, compromised the asymmetric enrichment of PIE-1:GFP before cell division (Table 1, X). Together, these data suggest that ZF2 participates in two separate processes: binding to P granules and, in combination with other sequences in region 3, asymmetric enrichment before cell division. Neither of these processes, however, is absolutely dependent on ZF2 (or ZF1). PIE-1:GFP lacking both ZF1 and ZF2 still exhibited a weak preference for germline blastomeres and weak binding to P granules in both *pie-1(+)* and *pie-1(0)* backgrounds (Table 1, Y).

Region 3 and ZF1 Are the Two Main Domains in PIE-1 Required for Segregation to the Germ Lineage

The analysis presented above identified two regions in PIE-1 required for localization to the germ lineage: region 3 and ZF1. To test whether other regions in PIE-1 might also contribute to asymmetry in the absence of these two domains, we constructed a PIE-1:GFP fusion lacking most of region 3 and with missense mutations in ZF1 (Table 1, Z). This fusion showed no preference

for germline blastomeres and was expressed at equal levels in all cells (Table 1, Z). We conclude that region 3 and ZF1 are the two main domains in PIE-1 responsible for localization to the germ lineage.

***par-1* Is Required to Inhibit ZF1-Dependent Degradation in Posterior Cells**

par-1 encodes a serine/threonine kinase required for the establishment of anterior/posterior polarity in the early embryo (Guo and Kemphues, 1995). In *par-1* mutants, all blastomeres divide equally and PIE-1 is partitioned equally to all cells up to the 4-cell stage (Tenenhaus et al., 1998). After that stage, PIE-1 rapidly disappears and is no longer detected in any cell. These observations suggested that the mechanism that degrades PIE-1 in somatic cells might still be active in *par-1* mutants. To test this possibility, we examined the distributions of wild-type PIE-1:GFP, PIE-1:GFP with a deletion in region 3 (PIE-1:GFPRegion 3Δ), and PIE-1:GFP with a deletion that removes ZF1 (PIE-1:

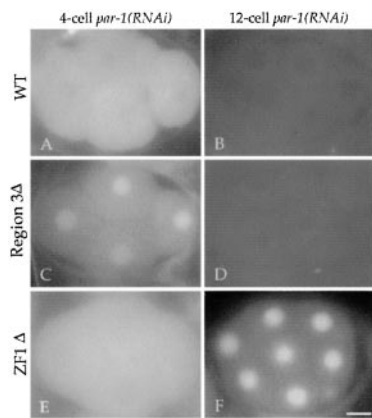


Figure 5. *par-1* Is Required to Block ZF1-Dependent Degradation in Posterior Blastomeres

(A–F) 4-cell (A, C, and E) and 12-cell (B, D, and F) *par-1* (RNAi) embryos expressing (A and B) wild-type PIE-1:GFP; (C and D) PIE-1:GFP with a deletion in region 3; (E and F) PIE-1:GFP lacking ZF1. Scale bar is 10 μm.

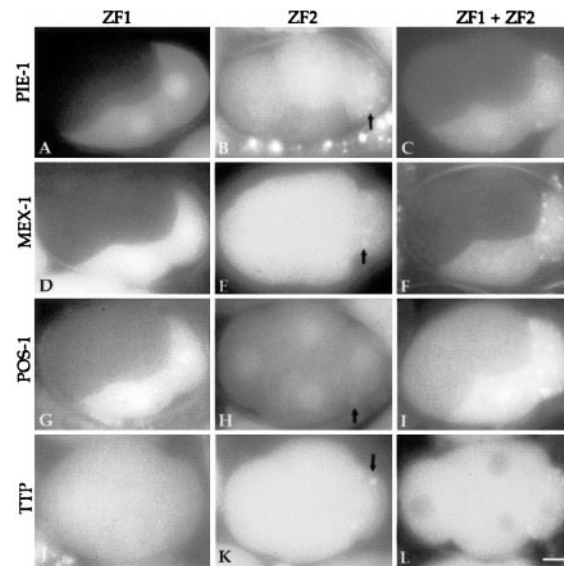


Figure 6. Localization Properties of CCCH Fingers from PIE-1, MEX-1, POS-1, and TTP

Four-cell embryos expressing ZF1:GFP, ZF2:GFP, and ZF1 + ZF2:GFP fusions from PIE-1, MEX-1, POS-1, and TTP as indicated. Arrows point to P granules in ZF2:GFP-expressing embryos. All fusions were uniformly distributed in the 1- and 2-cell stages (Figure 3C and data not shown). Scale bar is 10 μm.

GFPZF1 Δ) in animals where *par-1* activity was inhibited by RNA-mediated interference (RNAi). As expected, all three fusions were partitioned equally during the first two cleavages (Figures 5A, 5C, and 5E). After the 4-cell stage, wild-type PIE-1:GFP and PIE-1:GFPRegion 3 Δ quickly disappeared from all cells (Figures 5B and 5D). In contrast, PIE-1:GFPZF1 Δ continued to be maintained in all cells and could still be detected throughout the embryo past the 28-cell stage (Figure 5F and data not shown). These observations demonstrate that loss of PIE-1 in *par-1* mutants is dependent on ZF1 as it is in wild type. We conclude that *par-1* activity is not required for ZF1-dependent degradation and that in *par-1* mutants, ZF1-dependent degradation is active in all blastomeres.

ZF1-dependent degradation appears to have slower kinetics in *par-1* mutants compared to wild type. In *par-1* mutants, PIE-1:GFP can still be detected in the 4-cell stage (Figure 5A), whereas in wild-type embryos, PIE-1:GFP is eliminated from the AB lineage before the 4-cell stage (Figure 3B). This difference raises the possibility that *par-1* is required not only to exclude ZF1-dependent degradation from germline blastomeres but also to concentrate it in somatic blastomeres.

Localization Properties of CCCH Fingers

The two CCCH fingers in PIE-1 have different properties: ZF1 targets PIE-1 for degradation in somatic blastomeres, and ZF2 targets PIE-1 to P granules. CCCH fingers have also been described in MEX-1 and POS-1, two maternal proteins that, like PIE-1, segregate with the germ lineage in embryos (Guedes and Priess, 1997; Tabara et al., 1998). To test whether the MEX-1 and POS-1 fingers have properties similar to the PIE-1 fingers, we fused these fingers to GFP and examined their localization pattern *in vivo*. We found that, like PIE-1 ZF1, the ZF1s of MEX-1 and POS-1 were sufficient to target GFP for degradation specifically in somatic blastomeres (Figures 6A, 6D, and 6G). Similarly, like PIE-1 ZF2, the ZF2s of MEX-1 and POS-1 were sufficient to target GFP to P granules (Figures 6B, 6E, and 6H). Fusions containing both fingers exhibited both patterns (Figures 6C, 6F, and 6I).

We also analyzed by the same method the CCCH fingers of mammalian TTP (DuBois et al., 1990; Lai et al., 1990; Varnum et al., 1991). Unlike the other ZF1s we tested, TTP ZF1 was not sufficient to target GFP for degradation in somatic blastomeres; TTP-ZF1:GFP was maintained in all cells at equal levels (Figure 6J). Like the other ZF2s, however, TTP ZF2 was able to target GFP to P granules (Figure 6K).

Discussion

In *Drosophila* neuroblasts, determinants are segregated asymmetrically by associating with a specific region of the cell cortex (Jan and Jan, 1998). In *S. cerevisiae*, Ash1p is restricted to daughter cells by a cytoplasmic transport mechanism that localizes *ASH1* mRNA to emerging buds (Bobola et al., 1996; Chang and Drubin, 1996). In this study, we show that the PIE-1 employs yet another strategy to regulate its asymmetric distribution in *C. elegans* embryos. This strategy involves two complementary mechanisms: a first mechanism that acts in the mother cell to enrich PIE-1 in the cytoplasm

destined for the germline daughter, and a second mechanism that acts after cell division to degrade any PIE-1 left over in the somatic daughter.

PIE-1 Segregation to the Germ Lineage Depends Primarily on Mechanisms Acting at the Protein Level and Does Not Require Binding to Centrosomes

The presence of maternally encoded *pie-1* mRNA in embryos raised the possibility that PIE-1 asymmetry might be regulated at the RNA level. Our results, however, argue against this possibility. First, we found that noncoding sequences in the *pie-1* mRNA are neither necessary nor sufficient to localize PIE-1. Second, the two localization domains we identified in the *pie-1* open reading frame are functional when fused in-frame to GFP but not when fused out-of-frame. Third, missense mutations predicted to disrupt zinc binding by the CCCH fingers eliminated or reduced the localization properties of each domain. Together, these data indicate that PIE-1 asymmetry is regulated primarily by mechanisms acting on the PIE-1 protein rather than the *pie-1* RNA. Our results, however, do not exclude the possibility that RNA-based mechanisms are also functioning in parallel, perhaps to ensure that high levels of PIE-1 are maintained in germline blastomeres. Two lines of evidence support this possibility. First, *in situ* hybridization studies have shown that after the 4-cell stage *pie-1* mRNA is maintained only in germline blastomeres and is lost from somatic lineages (Tenenhaus et al., 1998). Second, as shown in this study, replacement of the *pie-1* 3' UTR with the *let-858* 3' UTR causes a reduction in PIE-1:GFP levels in germline blastomeres. These observations suggest that mechanisms acting on the *pie-1* RNA may exist to reinforce the asymmetry established by mechanisms acting on the PIE-1 protein. A similar situation has been described for *Drosophila* Prospero. In dividing neuroblasts, Prospero RNA, like Prospero protein, is targeted to a basal crescent during mitosis and is inherited preferentially by the basal daughter (Li et al., 1997; Broadus et al., 1998). Unlike asymmetric segregation of Prospero protein, asymmetric segregation of Prospero RNA is not essential and is only required when Prospero activity has been compromised (Broadus et al., 1998).

During mitosis, PIE-1 accumulates on centrosomes with a preference for the centrosome destined for the germline daughter. We have mapped the domain responsible for this localization down to a 21 amino acid region near the amino terminus of PIE-1. By itself, this domain can target GFP to mitotic centrosomes but shows no preference for germline centrosomes. Deletion of this domain eliminates binding to centrosomes but does not affect PIE-1's ability to segregate asymmetrically. We conclude that association with centrosomes is neither necessary nor sufficient for PIE-1 asymmetry. This finding is in agreement with the results of Schumacher et al. (1998), who showed that PIE-1 asymmetry is maintained in some embryos depleted for AIR-1, a centrosomal kinase essential for PIE-1's interaction with centrosomes.

PIE-1 Segregation Is Mediated by Two Complementary Mechanisms

We have identified two domains in PIE-1 required for asymmetric segregation in embryos. A first domain near the carboxyl terminus including PIE-1's second CCCH

finger is necessary and sufficient to enrich PIE-1 before cell division in the area of the cytoplasm destined for the next germline blastomere ("germline side"). Our observations of PIE:GFP fusion in live embryos indicate that in the 1-cell stage this enrichment results from both a decrease in PIE-1 levels in the anterior and an increase in PIE-1 levels in the posterior. This pattern is consistent with the possibility that PIE-1 moves from anterior to posterior. Alternatively, PIE-1 could be degraded locally in the anterior while also being translated throughout the entire cytoplasm. We attempted to address directly whether protein degradation and/or protein synthesis might be involved by treating embryos with proteasome inhibitors (MG 132 and LLnL) and with the protein synthesis inhibitor cycloheximide. These drugs eliminated PIE-1 asymmetry before cleavage but also completely blocked progression through the cell cycle (K. J. R. and G. S., unpublished data), making it difficult to identify any potentially direct effects on PIE-1. Although our data indicate that localized degradation contributes to PIE-1 asymmetry after cell division (see below), we do not yet know whether PIE-1 asymmetry before cell division is due to localized degradation, movement, or a combination of both.

Enrichment of PIE-1 on the germline side is not absolute; low levels remain on the somatic side at the time of cleavage. Time-lapse recording and quantitation of PIE-1:GFP levels over time reveal that these low levels are inherited by the somatic daughter but are not maintained in that cell. Surprisingly, we found that this loss depends on the first CCCH finger in PIE-1 (ZF1). Cys-to-Ser mutations in ZF1 stabilize PIE-1:GFP in somatic blastomeres and their descendants without significantly affecting PIE-1 asymmetry before cell division. Furthermore, fusion of ZF1 to GFP is sufficient to cause GFP to be degraded specifically in somatic blastomeres but is not sufficient to promote asymmetric enrichment before cell division. Since these data demonstrate that predivision enrichment and postdivision degradation can occur independently from one another and require different domains in PIE-1, we conclude that these two processes are mediated by distinct mechanisms.

Regulation of PIE-1 Asymmetry by PAR-1

How do the mechanisms that localize PIE-1 become polarized along the anterior/posterior axis? Establishment of anterior/posterior polarity in the zygote depends on the actin cytoskeleton and on a network of cortical proteins that become asymmetrically localized after fertilization (Rose and Kemphues, 1998). Among these, PAR-1 is essential for most asymmetries that appear in the cytoplasm of the zygote and its descendants. Consistent with the idea that the mechanisms that localize PIE-1 are dependent on the establishment of A/P polarity, both an intact cytoskeleton and PAR-1 are required for PIE-1 asymmetry (this study; Tenenhaus et al., 1998). PAR-1 localizes to the posterior cortex in the zygote and is segregated into P₁ during the first cleavage (Guo and Kemphues, 1995). Like PIE-1, PAR-1 initially is uniformly distributed in P₁ and becomes localized to the posterior (where P₂ will form) before cell division. Asymmetric segregation of PAR-1 is repeated in each germline blastomere. This dynamic localization pattern suggests the intriguing possibility that PAR-1 regulates PIE-1 asymmetry by creating a local environment where PIE-1 is protected from degradation. In support of this

possibility, we have found that in the absence of *par-1* activity, ZF1-dependent degradation is activated in all cells. Furthermore, PIE-1 is found in ectopic locations in *par-3* mutants where PAR-1 is mislocalized (Tenenhaus et al., 1998). How PAR-1, a putative serine threonine kinase enriched on the cortex, influences PIE-1 stability in the cytoplasm remains to be determined. Recently, the cytoplasmic protein MEX-5 and its closely related homolog MEX-6 have been shown to function downstream of PAR-1 to inhibit the expression of PIE-1 and other germline proteins in the anterior (Schubert et al., 2000). These findings raise the possibility that PAR-1 may affect PIE-1 stability indirectly by excluding MEX-5 and MEX-6 from the posterior end of the embryo.

Regulation of Protein Localization by CCCH Fingers

PIE-1 belongs to a large family of proteins characterized by two linked CCCH fingers (ZF1 and ZF2) (DuBois et al., 1990; Lai et al., 1990; Varnum et al., 1991; Ma et al., 1994; Warbrick and Glover, 1994; Mello et al., 1996; Thompson et al., 1996; Guedes and Priess, 1997; Stevens et al., 1998; Tabara et al., 1998; De et al., 1999; te Kronnie et al., 1999). CCCH fingers in several proteins have been implicated in binding to RNA. For example, in mammalian TTP, both ZF1 and ZF2 are required for sequence-specific binding to the TNF- α 3' UTR (Lai et al., 1990; Carballo et al., 1998). An RNA binding function is consistent with our finding that ZF2 in PIE-1 can associate with P granules, since P granules are rich in RNA (Seydoux and Fire, 1994; Pitt et al., 2000). Indeed, TTP ZF2 can also associate with P granules when expressed in *C. elegans* embryos. Similarly, ZF2s from MEX-1 and POS-1, two other CCCH proteins which, like PIE-1, segregate with the germ lineage (Guedes and Priess, 1997; Tabara et al., 1998), can also associate with P granules.

Unlike ZF2s, however, ZF1s from PIE-1, TTP, MEX-1, and POS-1 are not sufficient to bind P granules when fused to GFP. Instead, ZF1s from PIE-1, MEX-1, and POS-1 (but not TTP) target GFP for degradation specifically in somatic blastomeres. Our observations suggest that ZF1s are recognized by a degradation machinery specific to somatic blastomeres and that ZF1-dependent degradation may be a commonly used strategy to exclude certain proteins from somatic lineages. In the case of POS-1, ZF1-dependent degradation is likely to be the primary mechanism by which this protein becomes excluded from somatic lineages since, unlike PIE-1 and MEX-1, POS-1 shows little asymmetry before division (Tabara et al., 1998). Our data also demonstrate that ZF1s and ZF2s are not equivalent and are likely to have different functions. Sequence comparison of ZF1s and ZF2s across the family supports the idea that ZF1s and ZF2s belong to two related but distinct classes that have been conserved across species (G. S., unpublished observations). It will be interesting to determine whether this sequence conservation reflects functional conservation across the family as is suggested by our findings with PIE-1, MEX-1, and POS-1.

Experimental Procedures

Strains

Caenorhabditis elegans N2 variety Bristol was the wild-type parent of all strains. The following mutant strains were used: *smg-1(e1228)*, *him-2(e1065)*, *pie-1(zu154)*, *unc-25(e156)/qC1*, and *dpy-18(e364)pie-1(zu127)/eT1 let-500*. Strains were maintained using standard techniques as described in Brenner (1974).

Cloning

Sequence information from Y49E10 was used to PCR-amplify a 7.7 kb genomic clone containing the *pie-1* gene. Oligonucleotides 2430 bases upstream of the *pie-1* ATG and 3202 bases downstream of TAA were used as primers. GFP was fused to the PIE-1 open reading frame either immediately after the second ATG (codon 11; pJH3.99) or immediately before the TAA codon (pJH3.92). Both fusions gave identical GFP patterns in embryos and could rescue the maternal effect lethality of a *pie-1(0)* mutation (data not shown). Mutant derivatives of pJH3.99 (pJH4.40, pJH4.87, pJH4.91, pJH5.02, pJH5.43, pJH5.59, pKR1.38, pKR1.55, pKR1.75) and pJH3.92 (pKR1.39) were constructed by recombinant PCR using overlapping mutagenic oligos. Replacement of the *pie-1* 3' UTR with that of *let-858* was accomplished by replacing 524 bp directly downstream of the *pie-1* TAA with the *let-858* 3' UTR (Kelly et al., 1997).

Constructs pJH5.12, pKR1.43, pKR1.44, pKR1.45, pKR1.46, pKR1.57, pKR1.58, pKR1.59, pKR1.60, pKR1.69, pKR1.74, pKR1.78, and pKR1.8 were derived by cloning specific domains of PIE-1 downstream of GFP in a vector (pKR 1.42) that uses the *pie-1* promoter, enhancer, and 3' UTR to drive maternal expression of GFP in embryos (K. J. R., unpublished data).

The MEX-1, POS-1, and TTP fingers were amplified using oligonucleotides based on published sequences (DuBois et al., 1990; Worthington et al., 1996; Guedes and Priess, 1997; Tabara et al., 1998) and cloned into pKR1.42 for expression in embryos.

Transgenic Lines

All transgenic lines were generated using the complex array method of Kelly et al. (1997), which prevents transgene silencing in the adult germline. In the course of our experiments, we learned that growth at 25°C improves expression from complex arrays (S. Strome, personal communication and K. J. R., unpublished observations), so some transformants were grown at 25°C before scoring for GFP. The embryos inside a minimum of 6 Roller hermaphrodites were examined for each line. In all cases, lines transformed with the same construct exhibited identical patterns, although expression levels often varied significantly between lines. In most lines, GFP expression was maintained only for a few generations (3–4) before being silenced, although exceptional lines that remained GFP positive for more than ten generations were also recovered.

To examine transgenes in the absence of endogenous PIE-1, we either injected *pie-1 (zu154) unc-25 (e156)/qC1* animals with the transgene of interest, or alternatively, we crossed stable transgenic lines with *dpy-18(e364) pie-1(zu127)/eT1 let-500* or *pie-1 (zu154) unc-25 (e156)/qC1* animals. The resulting Dpy Rol or Unc Rol hermaphrodites were examined for GFP fluorescence. Only embryos 15-cell and younger were analyzed since later *pie-1(0)* embryos have lineage defects (Mello et al., 1992).

RNA-Mediated Interference (RNAi)

par-1 sense and antisense transcripts were generated from plasmid ZC22 (Guo and Kemphues, 1995) using the Megascript kit (Ambion). Double-stranded RNA (200 ng/ul) was microinjected into Roller adult hermaphrodites expressing the GFP construct of interest. Embryos within these adults were examined by fluorescence microscopy the next morning. As expected for loss of *par-1* activity, 99.8% (562/563) of these embryos failed to hatch (embryonic lethal).

Inhibitor Studies

Early 2-cell stage embryos expressing PIE-1:GFP were processed as described by Edgar (1995) to remove their eggshell and vitelline membrane. Embryos were then washed in simple embryonic growth media (SGM) (Shelton and Bowerman, 1996), placed onto slides in SGM with or without the inhibitor (0.01 mg/ml of Cytochalasin D or Nocadazole [Sigma]), and examined immediately using Nomarski optics. PIE-1:GFP localization was scored 10 min later. At that time in control embryos, AB had completed cleavage, and PIE-1 had become localized to the posterior of P₁.

Time-Lapse Microscopy and Fluorescence Quantitation

Embryos were mounted on agarose pads as described previously (Waddle et al., 1996) in a media recommended by Lois Edgar, University of Colorado (60 mM NaCl, 32 mM KCl, 3 mM Na₂HPO₄, 2 mM

MgCl₂, 2 mM CaCl₂, 5 mM HEPES [pH 7.2], 0.2% glucose). Time-lapse microscopy was performed on an Olympus Bmax 60F microscope using a MicroMax-512EBFT CCD from Princeton Instruments. For the single focal plane image series shown in Figure 1, Nomarski DIC and GFP epifluorescence images were collected every 5 s using a 60×, 1.4 NA UPlanApo objective and an additional 1.25× magnification. Exposure times were 0.3 s for GFP fluorescence and 0.1 s for Nomarski DIC. Images were acquired with custom software (Jimage4D, <http://hamon.swmed.edu/~jwaddle/jimage4d.html>) and appended into a single multi-image TIFF file using Scion Image for Windows NT (Scion Corporation).

To quantitate GFP fluorescence for the graphs shown in Figure 4, three-dimensional time-lapse imaging was performed on three embryos expressing wild-type PIE-1:GFP and three embryos expressing PIE-1:GFP with ZF1 mutated. Sixteen optical sections, each 1.5 microns apart (256 × 256 pixels at 0.22 micron/pixel) were collected every 60 s from the 2-cell stage to the 12-cell stage; exposure times were 0.25 s for both the fluorescence and the Nomarski DIC channels. In all cases, the raw pixel values were within the linear range of the CCD camera (0–4095). Using a custom program (EditView4D, J. Waddle, unpublished) the image data was subjected to the LLS-MAP deconvolution algorithm to assign out-of-focus light back to its point of origin (Gibson and Lanni, 1991; Preza et al., 1992a, 1992b; the LLS-MAP code was kindly provided by K. Doolittle of the Washington University Biomedical Computer Laboratory; <http://www.ibt.wustl.edu/bcl/xcosm/xcosm.html>). After deconvolution, the three-dimensional stacks were cropped to a cubic region that just bound the embryo or the EMS cell. Mean pixel values for GFP fluorescence in the entire embryo or in the EMS cell were calculated for each time point from the sum of the individual pixel values (GFP fluorescence) in the appropriate volume. To correct for autofluorescence, the mean fluorescence from an identically treated non-GFP-expressing embryo was subtracted from the values obtained for the GFP-expressing embryos. Microsoft Excel was used to plot the average (N = 3) fluorescence remaining at any time point relative to the birth of EMS. Error bars report the 95% confidence limits in the mean values. Start and end mean pixel values for the plots shown in Figure 4 were as follows: WT PIE-1:GFP, total embryo (17.36, 11.73); EMS (36.22, 10.28). ZF1 mutant, total embryo (40.99, 41.43); EMS (71.89; 60.55).

Acknowledgments

We thank Charlotte Schubert and Jim Priess for many insightful discussions and for sharing their unpublished results, Barbara Amann and Jeremy Berg for advice on CCCH fingers, Elaine Pinheiro and Chi Zhang for their help in the analysis of the MEX-1, POS-1, and TTP fingers, Jim Priess, Phil Beachy, and members of the Seydoux lab for comments on the manuscript, Barbara Amann and Mark Worthington for plasmid pMW79, and Ken Kemphues for plasmid ZC22. This work was supported by grants from the Packard Foundation and the National Institutes of Health (R01HD37407).

Received March 9, 2000; revised June 20, 2000.

References

- Bertrand, E., Chartrand, P., Schaefer, M., Shenoy, S.M., Singer, R.H., and Long, R.M. (1998). Localization of ASH1 mRNA particles in living yeast. *Mol. Cell* 2, 437–445.
- Bird, D.M., and Riddle, D.L. (1989). Molecular cloning and sequencing of *ama-1*, the gene encoding the largest subunit of RNA polymerase II. *Mol. Cell. Biol.* 9, 4119–4130.
- Bobola, N., Jansen, R.P., Shin, T.H., and Nasmyth, K. (1996). Asymmetric accumulation of Ash1p in postanaphase nuclei depends on a myosin and restricts yeast mating-type switching to mother cells. *Cell* 84, 699–709.
- Brenner, S. (1974). The genetics of *Caenorhabditis elegans*. *Genetics* 77, 71–94.
- Broadus, J., Fuerstenberg, S., and Doe, C.Q. (1998). Stufen-dependent localization of prospero mRNA contributes to neuroblast daughter-cell fate. *Nature* 391, 792–795.

- Carballo, E., Lai, W.S., and Blackshear, P.J. (1998). Feedback inhibition of macrophage tumor necrosis factor- α production by tristetraprolin. *Science* **281**, 1001–1015.
- Chalfie, M., Tu, Y., Euskirchen, G., Ward, W., and Prasher, D.C. (1994). Green fluorescent protein as a marker for gene expression. *Science* **263**, 802–805.
- Chang, F., and Drubin, D.G. (1996). Cell division: why daughters cannot be like their mothers. *Curr. Biol.* **6**, 651–654.
- C. elegans sequencing consortium (1998). Genome sequence of the nematode *C. elegans*: a platform for investigating biology. *Science* **282**, 2012–2018.
- De, J., Lai, W.S., Thorn, J.M., Goldsworthy, S.M., Liu, X., Blackwell, T.K., and Blackshear, P.J. (1999). Identification of four CCCH zinc finger proteins in *Xenopus*, including a novel vertebrate protein with four zinc fingers and severely restricted expression. *Gene* **228**, 133–145.
- Doe, C.Q., Chu-LaGriff, Q., Wright, D., and Scott, M. (1991). The prospero gene specifies cell fates in the *Drosophila* central nervous system. *Cell* **65**, 451–463.
- DuBois, R.N., McLane, M.W., Ryder, K., Lau, L.F., and Nathans, D. (1990). A growth factor-inducible nuclear protein with a novel cysteine/histidine repetitive sequence. *J. Biol. Chem.* **265**, 19185–19191.
- Edgar, L.G. (1995). Blastomere culture and analysis. *Methods Cell Biol.* **48**, 303–321.
- Evans, T.C., Crittenden, S.L., Kodoyianni, V., and Kimble, J. (1994). Translational control of maternal glp-1 mRNA establishes an asymmetry in the *C. elegans* embryo. *Cell* **77**, 183–194.
- Gibson, F.S., Lanni, F. (1991). Experimental test of an analytical model of aberration in an oil-immersion objective lens used in three-dimensional light microscopy. *J. Opt. Soc. Am. A* **8**, 1601–1613.
- Guedes, S., and Priess, J.R. (1997). The *C. elegans* MEX-1 protein is present in germline blastomeres and is a P granule component. *Development* **124**, 731–739.
- Guo, S., and Kemphues, K.J. (1995). par-1, a gene required for establishing polarity in *C. elegans* embryos, encodes a putative Ser/Thr kinase that is asymmetrically distributed. *Cell* **81**, 611–620.
- Guo, S., and Kemphues, K.J. (1996). Molecular genetics of asymmetric cleavage in the early *Caenorhabditis elegans* embryo. *Curr. Opin. Genet. Dev.* **6**, 408–415.
- Hirata, J., Nakagoshi, H., Nabeshima, Y., and Matsuzaki, F. (1995). Asymmetric segregation of the homeodomain protein Prospero during *Drosophila* development. *Nature* **377**, 627–630.
- Hird, S.N., Paulsen, J.E., and Strome, S. (1996). Segregation of germ granules in living *Caenorhabditis elegans* embryos: cell-type-specific mechanisms for cytoplasmic localization. *Development* **122**, 1303–1312.
- Hunter, C.P., and Kenyon, C. (1996). Spatial and temporal controls target pal-1 blastomere-specification activity to a single blastomere lineage in *C. elegans* embryos. *Cell* **87**, 217–226.
- Hyman, A.A., and White, J.G. (1987). Determination of cell division axes in the early embryogenesis of *Caenorhabditis elegans*. *J. Cell Biol.* **105**, 2123–2135.
- Jan, Y.N., and Jan, L.Y. (1998). Asymmetric cell division. *Nature* **392**, 775–778.
- Kelly, W.G., Xu, S., Montgomery, M.K., and Fire, A. (1997). Distinct requirements for somatic and germline expression of a generally expressed *Caenorhabditis elegans* gene. *Genetics* **146**, 227–238.
- Knoblich, J.A. (1997). Mechanisms of asymmetric cell division during animal development. *Curr. Opin. Cell Biol.* **9**, 833–841.
- Knoblich, J.A., Jan, L.Y., and Jan, Y.N. (1995). Asymmetric segregation of Numb and Prospero during cell division. *Nature* **377**, 624–627.
- Lai, W.S., Stumpo, D.J., and Blackshear, P.J. (1990). Rapid insulin-stimulated accumulation of an mRNA encoding a proline-rich protein. *J. Biol. Chem.* **265**, 16556–16563.
- Lasko, P. (1999). RNA sorting in *Drosophila* oocytes and embryos. *FASEB J.* **13**, 421–433.
- Li, P., Yang, X., Wasser, M., Cai, Y., and Chia, W. (1997). Inscuteable and Staufin mediate asymmetric localization and segregation of prospero RNA during *Drosophila* neuroblast cell divisions. *Cell* **90**, 437–447.
- Long, R.M., Singer, R.H., Meng, X., Gonzalez, I., Nasmyth, K., and Jansen, R.P. (1997). Mating type switching in yeast controlled by asymmetric localization of ASH1 mRNA. *Science* **277**, 383–387.
- Ma, Q., Wadleigh, D., Chi, T., and Herschman, H. (1994). The *Drosophila* TIS11 homologue encodes a developmentally controlled gene. *Oncogene* **9**, 3329–3334.
- Mello, C.C., Draper, B.W., Krause, M., Weintraub, H., and Priess, J.R. (1992). The pie-1 and mex-1 genes and maternal control of blastomere identity in early *C. elegans* embryos. *Cell* **70**, 163–176.
- Mello, C.C., Schubert, C., Draper, B., Zhang, W., Lobel, R., and Priess, J.R. (1996). The PIE-1 protein and germline specification in *C. elegans* embryos. *Nature* **382**, 710–712.
- Pitt, J.N., Schisa, J.A., and Priess, J.R. (2000). P granules in the germ cells of *Caenorhabditis elegans* adults are associated with clusters of nuclear pores and contain RNA. *Dev. Biol.* **219**, 315–333.
- Preza, C., Miller, M.I., Thomas Jr., L.J., and McNally, J.G. (1992a). Regularized method for reconstruction of three-dimensional microscopic objects from optical sections. *J. Opt. Soc. Am. A* **9**, 219–228.
- Preza, C., Miller, M.I., and Conchello, J.A. (1992b). Image reconstruction for 3-D light microscopy with a regularized linear method incorporating a smoothness prior. *Proc. SPIE* **1905**, 129–139.
- Pulak, R., and Anderson, P. (1993). mRNA surveillance by the *Caenorhabditis elegans* smg genes. *Genes Dev.* **7**, 1885–1897.
- Rose, L.S., and Kemphues, K.J. (1998). Early patterning of the *C. elegans* embryo. *Annu. Rev. Genet.* **32**, 521–545.
- Schlesinger, A., Shelton, C.A., Maloof, J.N., Meneghini, M., and Bowerman, B. (1999). Wnt pathway components orient a mitotic spindle in the early *Caenorhabditis elegans* embryo without requiring gene transcription in the responding cell. *Genes Dev.* **13**, 2028–2038.
- Schubert, C.M., Lin, R., de Vries, C.J., Palasterk, R.H.A., and Priess, J.A. (2000). MEX-5 and MEX-6 function to establish soma-germline asymmetry in early *C. elegans* embryos. *Mol. Cell* **5**, 671–682.
- Schumacher, J.M., Ashcroft, N., Donovan, P.J., and Golden, A. (1998). A highly conserved centrosomal kinase, AIR-1, is required for accurate cell cycle progression and segregation of developmental factors in *Caenorhabditis elegans* embryos. *Development* **125**, 4391–4402.
- Seydoux, G., and Fire, A. (1994). Soma-germline asymmetry in the distributions of embryonic RNAs in *Caenorhabditis elegans*. *Development* **120**, 2823–2834.
- Seydoux, G., Mello, C.C., Pettitt, J., Wood, W.B., Priess, J.R., and Fire, A. (1996). Repression of gene expression in the embryonic germ lineage of *C. elegans*. *Nature* **382**, 713–716.
- Shapiro, L., and Losick, R. (1997). Protein localization and cell fate in bacteria. *Science* **276**, 712–718.
- Shelton, C.A., and Bowerman, B. (1996). Time-dependent responses to glp-1-mediated inductions in early *C. elegans* embryos. *Development* **122**, 2043–2050.
- Sil, A., and Herskowitz, I. (1996). Identification of asymmetrically localized determinant, Ash1p, required for lineage-specific transcription of the yeast HO gene. *Cell* **84**, 711–722.
- Stebbins-Boaz, B., and Richter, J.D. (1997). Translational control during early development. *Crit. Rev. Eukaryot. Gene Expr.* **7**, 73–94.
- Stevens, C.J., Schipper, H., Samallo, J., Stroband, H.W., and te Kronnie, T. (1998). Blastomeres and cells with mesendodermal fates of carp embryos express cth1, a member of the TIS11 family of primary response genes. *Int. J. Dev. Biol.* **42**, 181–188.
- Strome, S., and Wood, W.B. (1982). Immunofluorescence visualization of germ-line-specific cytoplasmic granules in embryos, larvae, and adults of *Caenorhabditis elegans*. *Proc. Natl. Acad. Sci. USA* **79**, 1558–1562.
- Strome, S., and Wood, W.B. (1983). Generation of asymmetry and segregation of germ-line granules in early *C. elegans* embryos. *Cell* **35**, 15–25.
- Tabara, H., Hill, R.J., Mello, C.C., Priess, J.R., and Kohara, Y. (1998).

pos-1 encodes a cytoplasmic zinc-finger protein essential for germline specification in *C. elegans*. *Development* 126, 1–11.

Takizawa, P.A., Sil, A., Swedlow, J.R., Herskowitz, I., and Vale, R.D. (1997). Actin-dependent localization of an RNA encoding a cell-fate determinant in yeast. *Nature* 389, 90–93.

te Kronnie, G., Stroband, H., Schipper, H., and Samallo, J. (1999). Zebrafish CTH1, a C3H zinc finger protein, is expressed in ovarian oocytes and embryos. *Dev. Genes Evol.* 209, 443–446.

Tenenhaus, C., Schubert, C., and Seydoux, G. (1998). Genetic requirements for PIE-1 localization and inhibition of gene expression in the embryonic germ lineage of *Caenorhabditis elegans*. *Dev. Biol.* 200, 212–224.

Thompson, M.J., Lai, W.S., Taylor, G.A., and Blackshear, P.J. (1996). Cloning and characterization of two yeast genes encoding members of the CCCH class of zinc finger proteins: zinc finger-mediated impairment of cell growth. *Gene* 174, 225–233.

Vaessin, H., Grell, E., Wolff, E., Bier, E., Jan, L., and Jan, Y. (1991). Prospero is expressed in neuronal precursors and encodes a nuclear protein that is involved in the control of axonal outgrowth in *Drosophila*. *Cell* 67, 941–953.

Varnum, B.C., Ma, Q.F., Chi, T.H., Fletcher, B., and Herschman, H.R. (1991). The TIS11 primary response gene is a member of a gene family that encodes proteins with a highly conserved sequence containing an unusual Cys-His repeat. *Mol. Cell. Biol.* 11, 1754–1758.

Waddle, J.A., Karpova, T.S., Waterston, R.H., and Cooper, J.A. (1996). Movement of cortical actin patches in yeast. *J. Cell Biol.* 132, 861–870.

Warbrick, E., and Glover, D. (1994). A *Drosophila melanogaster* homolog of the TIS11 family of immediate early genes that can rescue a *cdr1 cdc25* mutant strain of fission yeast. *Gene* 151, 243–246.

Worthington, M.T., Amann, B.T., Nathans, D., and Berg, J.M. (1996). Metal binding properties and secondary structure of the zinc-binding domain of Nup475. *Proc. Natl. Acad. Sci. USA* 93, 13754–13759.